

## ADVANCES IN NANO THERMAL ANALYSIS OF COATINGS

L. T. Germinario\* and P. P. Shang

Eastman Chemical Company, Corporate Analytical Services, Kingsport, TN, 37662, USA

This article discusses AFM-based localized thermal analysis of crosslinked polymer coatings based on a recent breakthrough in nanoscale thermal probe technology. The addition of a thermal tip to a conventional AFM adds a new and valuable capability of spatially resolved thermal analysis to the AFM. It is particularly useful for thin films since it enables the measurement of transition temperatures (melting ( $T_m$ ) or glass ( $T_g$ )) on selected regions of the sample aiding in the identification and characterization of phases on the length scales approaching macromolecular dimensions. Examples include the monitoring of the softening point of automotive clearcoat systems, as a function of cure time and cure temperature and characterization of degradation and embrittlement of weathered acrylic-polyurethane coatings. Comparison of nano thermal analysis with bulk DSC and MDSC is made and its inherent advantages over DSC in analyzing surfaces, is demonstrated.

**Keywords:** atomic force microscopy, automotive coatings, localized thermal analysis, nanoscale thermal analysis, softening point, spatially resolved thermal analysis, thermal probes, weathering

### Introduction

Organic polymeric materials are widely used as coatings in a variety of markets and applications, primarily to improve surface properties, appearance and performance. These applications are becoming more sophisticated, and due to the multivariate nature of coatings, their decreased dimensions often produce layers of polymers having different properties. In addition, the viscoelastic nature of most polymers leads to a marked time and temperature dependence on performance [1].

Chemically crosslinked coatings have evolved as the materials of choice and are commonly employed as automotive clearcoats to protect against environmental influences and provide scratch, mar and chip resistance, as well as corrosion and solvent resistance, while still maintaining a high gloss and appearance [2]. The addition of chemical additives to improve photostability, coupled with variable crosslinking reactions, often produce heterogeneities ranging in size from nanometers to microns that are more susceptible to degradation [3, 4]. The atomic force microscope (AFM) has proven to be invaluable for not only imaging polymeric systems [5], but for probing tip/sample interactions, (as in phase imaging) for mapping mechanical (elasticity, hardness, etc.) and chemical properties [6, 7].

Recent breakthroughs have enabled the fabrication of thermal probes with end radius of ~20 nm [8] which enable the AFM to probe local thermal properties at a sub-100 nm size scale. The addition of

a thermal tip to a conventional AFM adds a new and valuable capability of spatially resolved thermal analysis to the AFM. It is particularly useful for thin films since it enables the measurement of transition temperatures (melting or glass) on selected spots of the sample aiding in the identification and characterization of the phases at the nanoscale [9].

This article covers the preliminary work on the application of sub-100 nm thermal analysis on crosslinked polymer coatings. Examples include the monitoring of the softening point of automotive clearcoat systems, as a function of cure time and cure temperature and characterization of degradation and embrittlement of weathered acrylic-polyurethane coatings. Comparison of nano thermal analysis with bulk DSC (differential scanning calorimetry) and MDSC (modulated DSC) is also discussed.

### Experimental

Experiments were performed using a Veeco Dimension 3000 AFM equipped with an Anasys Instruments (AI) nano-TA module and AI nanoscale thermal probes. The nano-TA probes are supplied attached to the standard Dimension 3000 AFM probe mount with wires connected to each leg of the nano-TA probe for facile connection to the nano-TA controllers. The nano-TA probes directly mount onto the base of the standard piezoelectric tube shown schematically in Fig. 1b. As a result, experiments can be conducted using the standard segmented photo-

\* Author for correspondence: germ@eastman.com

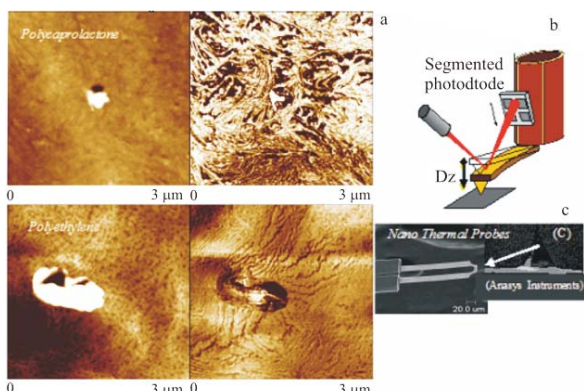


**Fig. 1** Example of test polymer film samples (polycaprolactone and polyethylene) used for calibration of nano thermal probes. a – height (left) and phase (right) images provide evidence of crystalline lamellar structure and spatial resolution comparable to standard AFM probes. c – nano thermal probes mount directly onto the b – dimension head

diode detector system supplied by the AFM microscope. The flow of current through the cantilever results in heat generation at the highly resistive heater region at the tip, while little heating occurs in the highly conductive legs. Each probe is calibrated by using it to identify the onset of known sharp melting points of various polymer standards (polycaprolactone, high density polyethylene and polyethylene-terephthalate). The heating rate used for this analysis was  $2^{\circ}\text{C s}^{-1}$  (though the nano-TA allows the probe heating rate to be controllably varied up to  $10000^{\circ}\text{C s}^{-1}$ ). All images were recorded using tapping mode AFM.

Sample surfaces are first scanned at ambient temperature to generate an image that is used to localize and define features of interest. The probe is next moved to select areas or features and the temperature of the stationary tip is then ramped linearly with time. This mode of analysis is referred to as local thermal analysis (LTA). As the probe is heated, the tip typically shows an increase in deflection due to local thermal expansion of the material beneath the tip (Fig. 1b). As the thermal transition is reached (glass transition temperature ( $T_g$ ), softening point or crystalline melting point ( $T_m$ )), the material softens beneath the tip and the probe forms an indentation as it penetrates the sample (Fig. 1a). This provides the nanoscale equivalent of a bulk thermo-mechanical analysis experiment. In order to confirm the tested points of interest, images are routinely recorded after performing the temperature ramp.

The nano-TA probes used in this study are the type more typically used for contact mode, and thus their resonance frequency was  $\sim 20$  kHz, while the typical resonant frequency for tapping mode tips

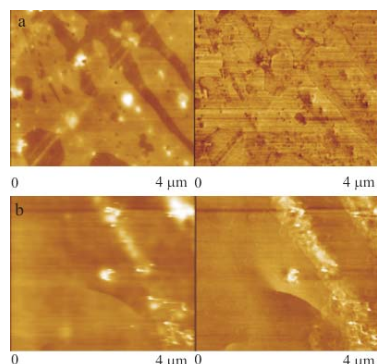


**Fig. 2** Example of resolution loss in images due to tip contamination most likely due to adhesion of molten polymer onto the nano-TA tip surface after conducting a LTA experiment. a – before LTA scan and b – after LTA scan

would be around 60 kHz. The probes were still capable of achieving height and phase images with sufficiently high spatial resolution to resolve polymer lamellar structures. Height images (Fig. 1a) often show the presence of mounds of material associated with indentations. This deposit is most likely polymeric material that collects and solidifies around the tip after performing a local thermal analysis. This buildup of polymer at the tip effectively increases the tip's diameter and leads to a loss in image resolution (Fig. 2). An example of this effect is displayed in the height and phase images in Fig. 2a. Surface features with sharp boundaries and interfaces are easily recognized on surface of a polyester film recorded at room temperature. Images recorded from the same region displayed in Fig. 2a, after performing a LTA experiment produced images (Fig. 2b) with a significant loss in resolution, as the images lack the sharp features observable in Fig. 2a. Repeated imaging with nano-thermal tips after performing a LTA experiment eventually restored the tip's original image resolution. This process of imaging regions after performing local thermal analysis was found to be useful for both examining the condition of the probe and for cleaning probes.

Two types of coatings were studied, (A) commercial acrylic polyol crosslinked with diisocyanate resin, catalyzed with di-butyl-tin-di-lauroate (DBTDL) and cured 30 min at  $60^{\circ}\text{C}$ ; and (B) weathered acrylic-polyurethane (AU) coatings. The weathered AU coatings consist of styrene-acrylic polymer cross-linked with polymeric 1,6-hexamethylene diisocyanate and containing two types of  $\text{TiO}_2$  particles,  $\text{TiO}_2$  pigment A, (average particle size  $\approx 20$  nm; uncoated and high photoactivity) and  $\text{TiO}_2$  pigment B, (average particle size  $\approx 250$  nm; coated with  $\text{Al}_2\text{O}_3$  (6%).

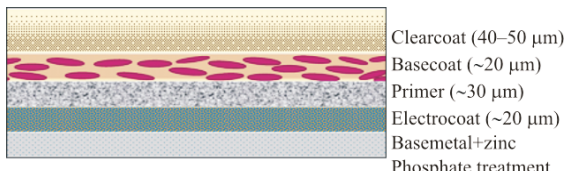


**Fig. 3** Cross-sectional view of typical automotive coating

## Results and discussion

A cross-sectional view of a typical commercial automotive coating (Fig. 3) shows the complex, multi-functional nature of these coating systems. Due to the fact that the clearcoat is the first line of defense against environmental influences, understanding surface, near-surface chemical and mechanical property development as a function of composition, cure time and environmental exposure is fundamental to improving their performance. Furthermore, the increased demand for low volatile organic compounds (VOC) systems in automotive refinish industry places greater demands for attaining fast cure at ambient temperature in order to reduce the investment in drying equipment and the time of repair.

Figure 1 shows the ambient temperature tapping mode images of polyethylene and polycaprolactone films with the thermal probes and the resolution is clearly comparable to regular non-thermal AFM probes. The thermal response of the probes was next investigated using acrylic-urethane coatings. Coatings that were a few weeks old were tested by LTA in order to measure the coating's response to a thermal scan and determine the indentation morphology and depth (Fig. 4).

The residual indentation produced by the thermal probe after measurement of softening point of an acrylic clearcoat film is shown in Fig. 4. Section analysis of the height image in Fig. 4 was performed in order to measure the indentation depth (~350 nm) and depression made by the nano-TA tip after the LTA experiment. The measured indentation depth provides an estimation of the sampling depth using LTA analysis and can serve as a basis for comparison of softening points ( $T_g$ ) from the same coatings with bulk film measurements by MDSC.

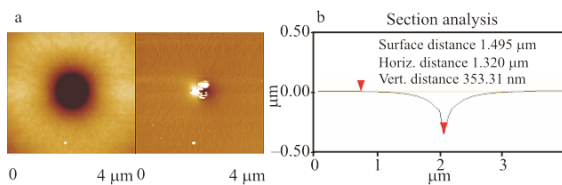


**Fig. 4** Topview images of the acrylic coating after LTA testing shows the formation of a residual indent ~350 nm deep when analyzed performing a section analysis (dotted line)

The dependence of the glass transition temperature on heating and cooling rates is well known and shown to be a kinetic effect that is due to a temperature dependence of structural relaxation rates. This temperature dependence also influences the shape of the heat capacity ( $C_p$ ) near the  $T_g$  [10]. In particular, experimental measurements showed  $T_g$  to depend linearly with the logarithm of the heating rate. In order to test the ability of LTA to measure a heating rate dependence of softening temperature using thermal probes, experiments were conducted on acrylic clearcoat films (Fig. 5a). The three scan rates tested, (6, 10 and 120°C min<sup>-1</sup>) by LTA clearly show an increase in softening temperature with increased heated rates and a linear logarithmic rate dependence (RSquare=0.999), similar to that shown by the bulk DSC measurement (Fig. 5b).

We next explore use of LTA for measuring cure rates from softening temperature. A coating's softening point is a good measure of crosslink density [11]. The formation of three-dimensional networks due to chemical reactions is widely accepted as a means of improving a coating's properties. It has been shown on a variety of clearcoat systems (1 and 2 K solvent-borne clearcoat, and 1 and 2 K waterborne clearcoat)

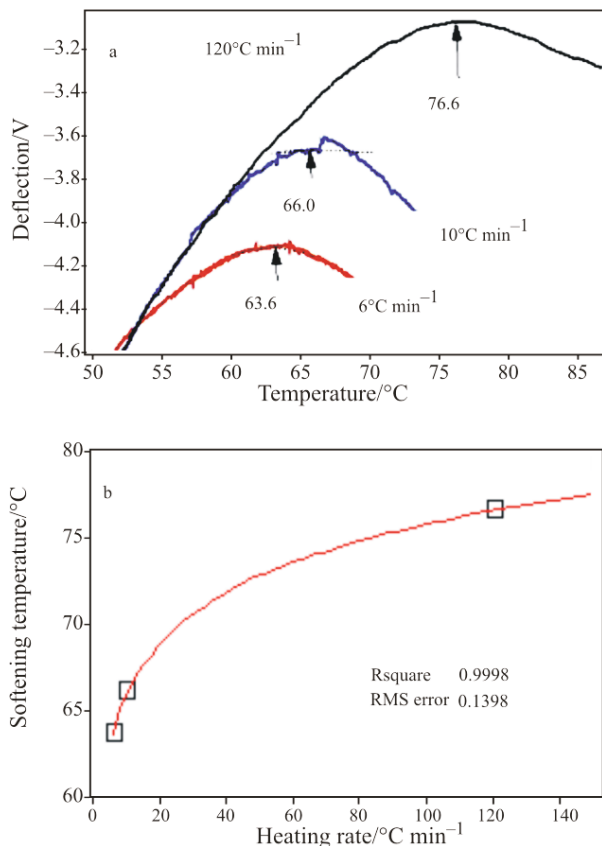
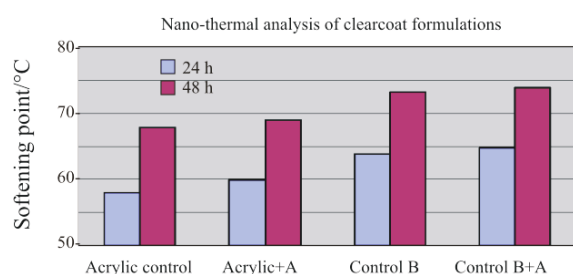


**Fig. 5** a – dependence of (acrylic) film softening point on tip heating rate. b – in particular, softening point onset temperature shows a linear dependence on the logarithm of the tip heating rate

**Table 1** Increase in softening temperatures as a function of time, 24 and 48 h, for select acrylic coatings

	Acrylic control	Acrylic+A	Control B	Control B+A
Tested for 24 h				
Nano-thermal AFM	57.6	60.3	63.7	64.8
Onset softening temp./°C	58.1	59.8	63.8	64.7
	58.0	59.4	63.8	64.9
Average	57.9	59.9	63.8	64.8
Standard dev.	0.3	0.4	0.0	0.2
Tested for 48 h				
Nano-thermal AFM	68.2	68.9	73.0	73.8
Onset softening temp./°C	67.9	68.8	73.1	73.9
	67.5	69.1	73.5	74.0
Average	67.9	68.9	73.2	73.9
Standard dev.	0.4	0.2	0.2	0.1



cured at different times, at different temperatures, all displayed an increase in  $T_g$ , with increasing crosslink density [12]. In addition, mechanical properties of coatings also depend on the extent of crosslinks as expressed by the inverse relationship between molecular mass between crosslinks ( $M_x$ ) and tensile storage modulus ( $E'$ ).

$$E' = 3nRT/M_x \quad (1)$$

where  $n$  is the density,  $R$  the gas constant and  $T$  the absolute temperature.

In order to test the utility of LTA for measuring cure (crosslinking) rates, softening points of commercial acrylic coatings cured for 30 min at 60°C, were tested from 2 to 72 h, after the 30 min bake at 60°C. Figure 6 shows a gradual increase in measured softening temperature with time. A plot of cure time vs. softening temperature shows a linear relationship over the cure times measured. The slope of this line is a measure of cure or crosslinking rates.

We next proceeded to use LTA to follow the increase in softening temperature (and crosslink density) as a function of time, 24 and 48 h, to select acrylic coatings after their 30 min bake at 60°C (Table 1). Pooling of the measured standard deviations of softening points, made in triplicate, from eight coating systems provided a good measure of the

LTA test reproducibility. The calculated standard deviation for these coating is 0.26°C (Table 1).

#### Photo-degraded acrylic-polyurethane (AU) coatings

These coatings were exposed, 20 and 41 weeks to UV-A and UV-B. They consist of styrene-acrylic polymer crosslinked with 1,6-hexamethylene diiso-

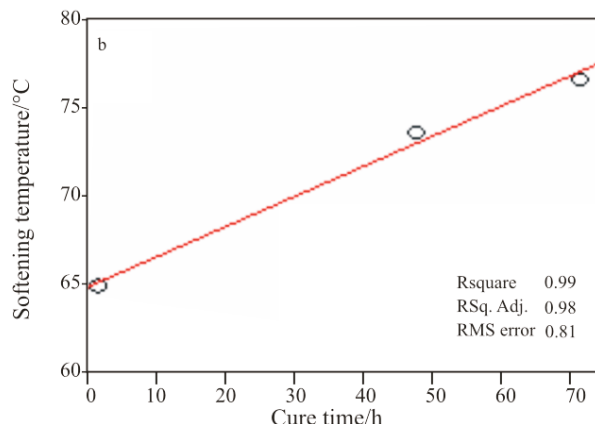
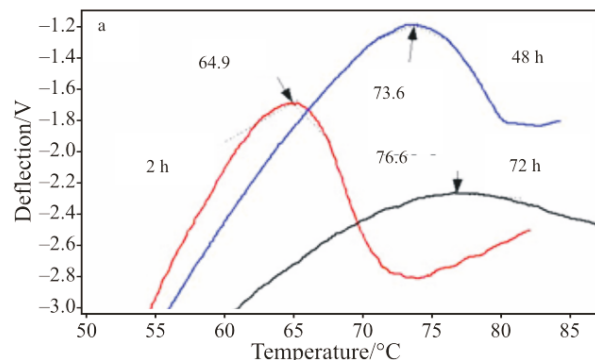


**Fig. 6** a – effect of curing (crosslinking) time at ambient temperature of acrylic clearcoat on softening temperature. b – the softening temperature displays a linear relationship over the cure times measured

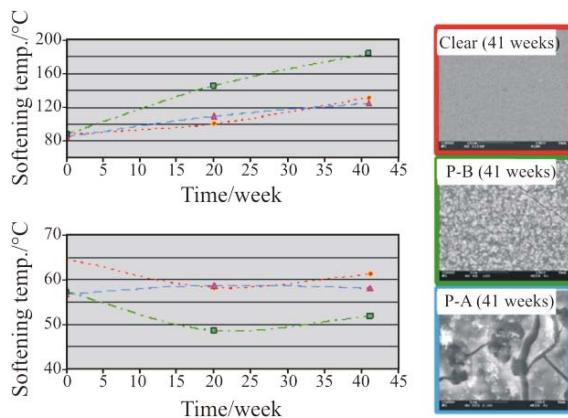


**Fig. 7** Comparison of softening temperatures measured for UV-exposed (0, 20 and 41 weeks) clear and  $\text{TiO}_2$  filled (P-A and P-B) acrylic urethane coatings using a – nano thermal analysis and b – MDSC. Surface morphology was also analyzed by scanning electron microscopy

cyanate and contain two types of  $\text{TiO}_2$  particles,  $\text{TiO}_2$  pigment A (P-A) (average particle size  $\approx 20$  nm; uncoated and highly photoactive) and  $\text{TiO}_2$  pigment B (P-B) (average particle size  $\approx 250$  nm; coated with  $\text{Al}_2\text{O}_3$  (6%)). Figure 7 summarizes and compares softening temperatures measured by LTA (Fig. 7a), in comparison with  $T_g$  from MDSC, (Fig. 7b). Scanning electron micrographs (SEM) are included to show the surface pitting and topography that develops as a result of photodegradation and volatilization of the acrylic-polyurethane coating. This spatial information is lost by the MDSC experiments as these methods can only measure an averaged response and cannot differentiate chemical inhomogeneities on or within the coating.

These data clearly show the surface sensitivity of LTA, as compared to the bulk  $T_g$  measurement using MDSC. A considerable body of knowledge has accumulated on the surface sensitivity of photodegradation processes [13]. It is therefore not surprising that NTA provides a sensitive measure of photooxidative effects of UV exposure for clear and  $\text{TiO}_2$ -filled coatings and displays an increase in softening temperature (i.e. crosslink density) with increased UV exposure times. In comparison, the MDSC characterization of the bulk thin film is not

capable of differentiating surface effects from bulk and cannot detect the surface chemical and structural degradation suffered by coatings as shown by the scanning electron micrographs from 41 week exposed coatings (Fig. 7).

## Acknowledgements

The authors express their gratitude to Drs Aaron Forster and Stephanie Watson (NIST) for valuable discussions and supply of weathered, acrylic-polyurethane coatings. We also thank Dr. Deepanjan Bhattacharya and Mr. Chip Williams for supply of acrylic clearcoats.

## References

- 1 L. C. E. Struik, *Physical Aging of Amorphous Polymer and other Materials*, Elsevier, Amsterdam 1978.
- 2 E. V. Schmidt, *Exterior Durability of Organic Coatings*, FMJ Intern. Publ., Redhill Surrey 1988.
- 3 H. Corti, R. Fernández-Prini and D. Gómez, *Prog. Org. Coat.*, 10 (1982) 5.
- 4 C.-I. Wu, X.-J. Zhou and Y.-J. Tan, *Prog. Org. Coat.*, 25 (1995) 379.
- 5 S. N. Magonov, V. Elings and M.-H. Whangbo, *Surf. Sci.*, 375 (1997) L385.
- 6 S. N. Magonov, J. Cleveland, V. Elings, D. Denley and M.-H. Whangbo, *Surf. Sci.*, 389 (1997) 201.
- 7 G. Haugstad and R. R. Jones, *Ultramicroscopy*, 76 (1999) 77.
- 8 W. P. King, T. Kenny, K. Goodson, G. Cross, M. Despont, U. Durig, H. Rothuizen, G. Binning and P. Vettiger, *Appl. Phys. Lett.*, 78 (2001) 1300.
- 9 B. A. Nelson and W. P. King, *Rev. Sci. Instrum.*, 78 (2007) .
- 10 G. S. Grest and M. H. Cohen, *Phys. Rev. B*, 21 (1980) 4113.
- 11 D. J. Skrovanek and C. K. Schoff, *Prog. Org. Coat.*, 16 (1988) 135.
- 12 W. Schlesing, M. Buhk and M. Osterhold, *Prog. Org. Coat.*, 49 (2004) 197.
- 13 D. R. Fagerburg, ‘Weathering of Polyester and Copolyester Sheeting’ Atlas School of Natural and Accelerated Weathering, Miami, FL, April 28, 1999.

DOI: 10.1007/s10973-007-8922-x